Analytica Chimica Acta 1228 (2022) 340334

Contents lists available at ScienceDirect

Analytica Chimica Acta

journal homepage: www.elsevier.com/locate/aca

# A sensitive biosensor for ochratoxin A detection based on triple-helix aptaswitch and bioorthogonal capture enabled signal amplification

Mingzhen Zhu [a,b], Wei Yang [a], Hui Zhi [a], Changxin Huangfu [a,b], Xiaobo Zhang [a,b], Liang Feng [a,*]

[a] Department of Instrumentation and Analytical Chemistry, CAS Key Laboratory of Separation Science for Analytical Chemistry, Dalian Institute of Chemical Physics, Chinese Academy of Sciences, 457 Zhongshan Road, Dalian, 116023, PR China
[b] University of Chinese Academy of Sciences, Beijing, 100049, PR China

## HIGHLIGHTS

- The dexterous combination of **the triple-helix aptaswitch** and **signal amplification of the functionalized paper**.
- **Bioorthogonal capture-based signal amplification** enabled a **simple and cost-effective** detection platform.
- **General applicability**: variable aptamer sequence in the aptaswitch without redesigning the triple-helix structure.
- An ultrasensitive OTA determination platform: the limit of **0.026 ng/mL** with a linear range of **0.03–50 ng/mL**.
- **A reinforced selectivity, binding affinity, and sensitivity** with the usage of triple-helix aptaswitch in the biosensor.

## GRAPHICAL ABSTRACT

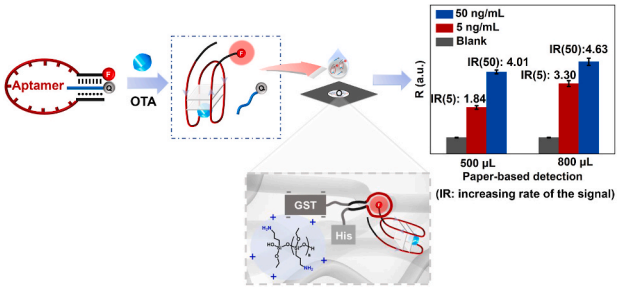


## ARTICLE INFO

*Keywords:*
OTA detection
Sensitive biosensor
Triple-helix aptaswitch
Bioorthogonal capture
Signal amplification

## ABSTRACT

Ochratoxin A (OTA) has been classified as a possible human carcinogen and accurate monitoring of OTA is crucial for avoiding the contaminant risk. Herein, a sensitive biosensor for OTA detection was reported. This biosensor achieved a lower detection limit of 0.026 ng/mL with the linear range of 0.03–50 ng/mL, owning to the coordination of the structure-switching of the aptaswitch and bioorthogonal capture-based signal amplification of the functionalized paper. Finally it was applied in real samples precisely and a portable device was developed for the easy readout of the fluorescent signal. Notably, this approach possessed adequate simplicity with the thorough avoidance of fluorescence plate reader or complicated material modification steps for signal amplification, and it was universally applicable by replacing the aptamer sequence in the loop instead of redesigning the structure of triple-helix aptaswitch for multifarious target analytes. Taken together, we first combined the triple-helix aptaswitch and bioorthogonal capture-based signal amplification in the detection of OTA, and this novel detection method may offer a simple, cost-effective and sensitive sensing platform for agricultural products quality monitoring.

* Corresponding author.
*E-mail address:* fengl@dicp.ac.cn (L. Feng).

https://doi.org/10.1016/j.aca.2022.340334
Received 9 July 2022; Received in revised form 9 August 2022; Accepted 26 August 2022
Available online 3 September 2022

## 1. Introduction

Ochratoxin A (OTA) is a typical representative of mycotoxin secreted by several species, including *Fusarium, Penicillium and Aspergillus* [1]. OTA contaminant occurs on a wide range of foods and has been considered as one of the most potential carcinogens (group 2B) [2–4]. Consequently, many countries have established strict limits on OTA levels [5,6]. In recent years, many sensitive detection platforms have been developed for the OTA monitoring. Conventional chromatographic methods, such as high-performance liquid chromatography (HPLC) coupled with fluorescence detector or mass spectrometry are the common analytical techniques for OTA analysis. However, the time-consuming methods require expensive equipments and tedious sample pretreatment, extremely hampering its practical applications in real samples [7–9]. Other than advanced instrumental analysis, enzyme-linked immunosorbent assay (ELISA) has also been used for OTA screening. Although high sensitivity is achieved, it has a challenge in matrix interference, cross reaction and stability issues of antibody in storage [10,11]. Thus, there is still an urgent demand for a simple, cost-effective and sensitive method to the detection of OTA in practical applications.

In recent years, aptamer-based biosensors have drawn significant attention. Comparing to antibody, aptamers have several significant advantages, including easy synthesis, easy storage and easy modification [12–14]. Moreover, based on the structure-switching during the target-aptamer binding event, many molecular engineering strategies such as molecular beacon and various molecular switch have been developed [15–18]. Noteworthy, among these molecular engineering strategies, triple-helix molecular switch has garnered increasing attention, which consists of a specific aptamer sequence with two arm-like fragments flanking by the sides of the aptamer and a dual-labeled triplex-forming oligonucleotide [18,19]. The special structure of triple-helix DNA maintains the stability, affinity and specificity of the original aptamer towards the targets, and even enables reinforced sensitivity [18,20,21]. In addition, it is generalizable with the aptamer sequence replaced in the loop instead of changing the triple-helix structure for various targets [22]. Given these virtues, the triple-helix DNA has great advantages in target recognition, and has been applied in the OTA detection platform with the binding constant (Kd) of 0.2 μM for the aptamer and OTA [23]. For instance, He et al. developed a triple-helix molecular switch and demonstrated a detection limit of 4 ng/mL in colorimetric mode [24]. Wang et al. described a triple-helix aptamer probe enabled chemiluminescence biosensor for OTA with a detection limit of 0.07 ng/mL [22]. Nevertheless, most of them were insensitive, which has been relatively problematic in the practical application. Thus, achieving a sensitive and simple assay for the detection of OTA is imperative.

Recently, a series of signal amplification strategies have been developed to realize ultrasensitive determination of OTA in aptamer-based biosensors. The most common strategy to transduce and amplify signals was through DNA amplifcation, including rolling circle amplifcation (RCA) [25], loop-mediated isothermal amplification (LAMP) [26], *etc*. In other instances, bioenzymes or nanomaterials were usually labeled on the probes for ultra-sensitivity [27,28]. However, the multiple enzymes or complicated modification involved in these operations limited the application of these amplification strategies. Recently, our group has reported a novel signal amplification strategy enabled by GST-TR512 fusion protein functionalized paper [29]. The functionalized paper retained the bioorthgonal capture of TR512-peptide towards Texas red fluorophore labeled oligonucleotide, realizing the enrichment of the signal probe evidently. Theoretically, this functionalized paper can provide a direct solution to the signal amplification with an enzyme-free and label-free process, resulting a simple, cost-effective and sensitive detection platform for OTA.

Inspired by these, we developed a novel triple-helix aptaswitch based biosensor for OTA detection with the combination of bioorthgonal capture-based signal amplification of the functionalized paper (Scheme 1). Upon the addition of OTA, the aptaswitch was opened by target recognition with the aptamer sequence in the loop of the triple-helix, resulting in the formation of an OTA-antiparallel G-quadruplex (OTA-AFDNA) complex with the increasing fluorescence intensity. Moreover, the signal would be further amplified by the bioorthogonal capture of Texas red fluorophore labeled oligonucleotide (namely OTA-AFDNA complex) on the GST-TR512 fusion protein functionalized paper. The obtained aptaswitch-based biosensor showed a lower detection limit of 0.026 ng/mL with the detection range of 0.03–50 ng/mL (the detection volume was 800 μL), improving the increasing rate (IR) of signal remarkably. Additionally, the biosensor was applied in real samples with good accuracy and precision. Finally, a portable device was developed for the easy readout of the fluorescent signal. Taken together, with the dexterous coordination of the triple-helix aptaswitch and bioorthogonal capture-based signal amplification of the functionalized paper, we may offer a simple, cost-effective and highly sensitive platform for practical detection of OTA in agricultural products quality monitoring.

## 2. Results and discussion

### 2.1. Analytical principle

The principle of the detection method is illustrated in Scheme 1. The triple-helix aptaswitch consisted of an OTA aptamer loop (in red), two fragment stems flanked by the sides of the aptamer (in black) labeled with Texas red fluorophore at the 3′-end (AFDNA), and an oligonucleotide matched with the stem (in blue) modified with BHQ2 at the 5′-end (QDNA) (the detailed information was in Fig. S1 in the Supporting Information (SI)). In the absence of OTA, the triple-helix aptaswitch was self-assembled via Watson-Crick and Hoogsteen base pairings, resulting in the nearly complete quenching of the fluorescent signal [30]. While in the presence of OTA, the aptaswitch would be opened by target recognition, resulting in the formation of OTA-antiparallel G-quadruplex (OTA-AFDNA) complex and the increasing of fluorescence intensity. Hence, the generated fluorescent signal could be correlated with OTA concentration.

To promote the performance of this aptaswitch, we introduced GST-TR512 fusion protein functionalized paper. The core part of the functionalized paper was the TR512-peptide in the fusion protein electrostatically immobilized on the paper, which could bioorthogonally capture Texas red fluorophore with high affinity ($K_d$ = 25 pM [31]) (Fig. S2 in the SI, the detailed information of the GST-TR512 fusion protein was in Fig. S3). Thus, the Texas red fluorophore labeled oligonucleotide (namely OTA-AFDNA complex) released in the aptaswitch was bioorthogonally captured on the functionalized paper, resulting in the signal amplification (Fig. S4 in the SI). In a word, using this sensing platform, a highly sensitive and simple biosensor for the detection of OTA would be developed.

### 2.2. Feasibility of the biosensor

The success of this work relied on the conformational transition of the triple-helix aptaswitch coupled with fluorescence enhancing primarily. Toward this end, we analyzed the fluorescence spectra and circular dichroism (CD) spectra of different kinds of samples. As shown in Fig. 1a and b, the triple-helix aptaswitch displayed a low background signal and a significant negative peak at 207 nm (curve 1), which was characteristic of the triplex-helix “hall mark” conformation [32]. These results indicated that the triple-helix structure was self-assembled successfully. In addition, there was no significant change of fluorescent signal in 6 h, ensuring the stability of the triple-helix structure (Fig. S5 in the SI). The aptaswitch produced a significant fluorescence enhancement in the presence of OTA (curve 2). In the meantime, a positive peak at 290 nm and a negative peak at 265 nm were observed corresponding

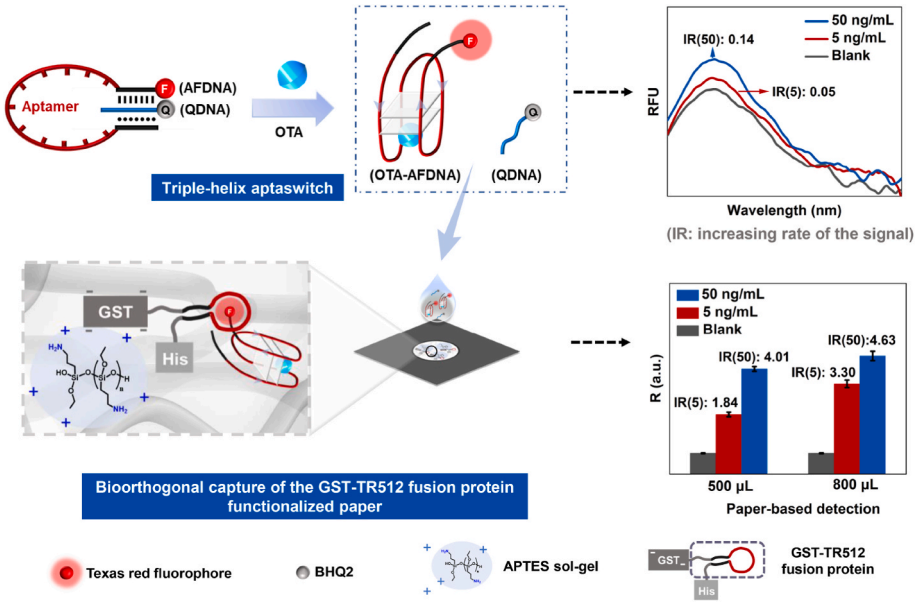


**Scheme 1.** Schematic representation of the triple-helix aptaswitch based biosensor. The Texas red fluorophore labeled oligonucleotide (namely OTA-AFDNA complex) released in the triple-helix aptaswitch was bioorthogonally captured on the GST-TR512 fusion protein functionalized paper, resulting an improvement in the increasing rate (IR) of signal remarkably.

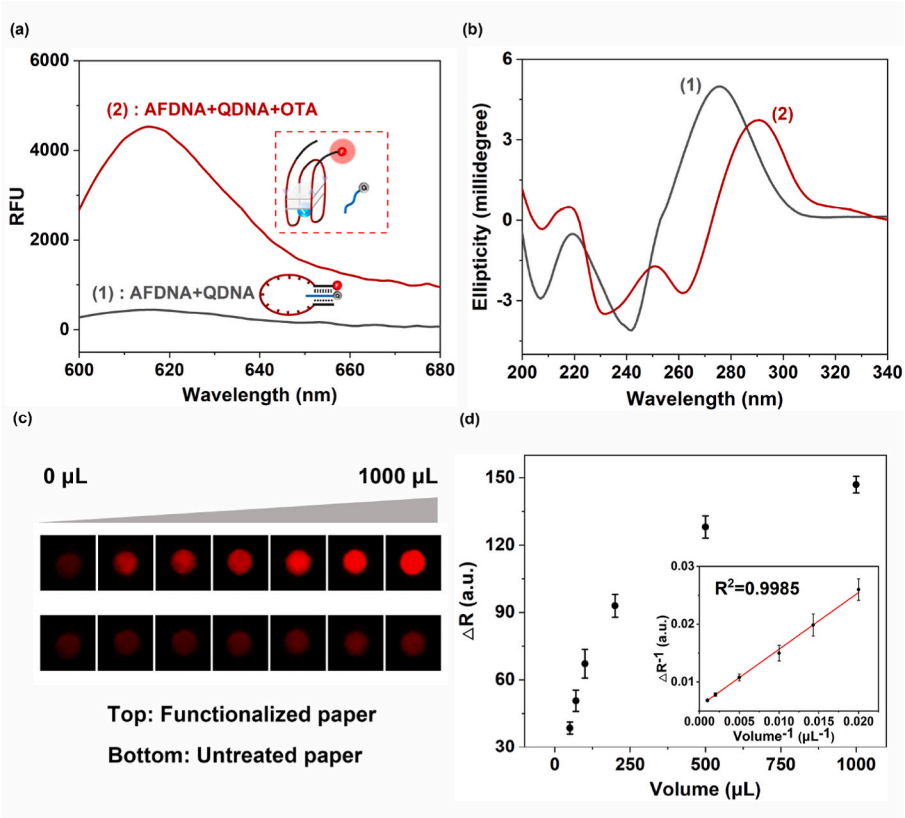


**Fig. 1.** The feasibility of the biosensor. Fluorescence spectra (a) and circular dichroism spectra (b) of different kinds of samples in the triple-helix aptaswitch. (c) the fluorescence intensity signal of functionalized paper and the untreated paper upon the increasing volume of Texas red labeled oligonucleotide solution (TR-ATCG, 0.1 μM). The paper-based detection was performed in a homemade chamber with a LED of 570 nm (Fig. S9 in the SI). The images were digitally quantified in (d). R was the red fluorescence response digitally quantified and ΔR meant the signal of R subtracted the signal of background $R_0$. Error bars: standard error (n = 3). (For interpretation of the references to color in this figure legend, the reader is referred to the Web version of this article.)

to the antiparallel G-quadruplex [33]. These phenomenons indicated that triple-helix structure was disassembled and the antiparallel G-quadruplex structure came into being by the recognition of OTA meanwhile. The fluorescence spectra and CD spectra of AFDNA was shown in Fig. S6 in the SI. Additionally, the structure-switching of the triple-helix aptaswitch was confirmed by polyacrylamide gel electrophoresis (Fig. S7 in the SI). Thus, the feasibility of the aptaswitch based on the triple-helix structure switching was proved with the fluorescence intensity changes as the important indicator for the quantification of OTA.

Furthermore, we confirmed the GST-TR512 fusion protein functionalized paper could quantitatively enrich Texas red fluorophore (TR) labeled oligonucleotide (TR-ATCG) for the signal amplification in the aptaswitch mentioned above. Through TR512-peptide based analyte

enrichment on the functionalized paper, a double reciprocal calibration curve $\Delta R^{-1} = 0.9827\ V^{-1}+0.0058$ ($R^2 = 0.9985$) was obtained (Fig. 1c and d). However, the increasement of the ΔR on the untreated paper was negligible (Fig. 1c and Fig. S8 in the SI). This demonstrated the functionalized paper could capture Texas red fluorophore labeled oligonucleotide effectivity, indicating its potential in the quantitative analysis of OTA-AFDNA complex released in the aptaswitch of the OTA detection platform.

### 2.3. Optimization of experimental conditions for the triple-helix aptaswitch

Some optimal conditions were identified to achieve the high performance of the triple-helix aptaswitch, including triple-helix stem length, ratio of QDNA to AFDNA, time and temperature for the triple-helix self-assembly, time and temperature for the target recognition, and the pH of binding buffer. The increasing rate (IR) of arbitrary fluorescence units (RFU) ($IR=(RFU-RFU_0)/RFU_0$) was used to determine the optimized parameters when it came to the recognition of OTA, where RFU and $RFU_0$ represented the fluorescent signal at 615 nm in the presence and absence of OTA with the fluorescence plate reader, respectively.

Firstly, The length of triple-helix stem was crucial for the structure-switching aptaswitch with T-A•T and C-G•$C^+$ base triplets [34]. The overlong or too short length of the triple-helix stem either prevented the open of the aptaswitch by the OTA recognation or yielded an unacceptable background signal. Toward this end, a series of triple-helix structures with different lengths of stem (from 6 nt to 10 nt, with AFDNA6 to AFDNA10, QDNA6 to QDNA10, Table S1 in the SI) were investigated. As shown in Fig. 2a and b, the highest IR was observed in the stem length of 7 base pairs, providing a good balance of low background signal and high sensitivity. And thus, 7 base pairs in the stem length were used for all subsequent experiments.

Secondly, the ratio of QDNA to AFDNA was evaluated with a constant concentration (2 μM) of AFDNA. The optimum performance was achieved at a molar ratio of 2:1. Therefore, the QDNA to AFDNA ratio of 2:1 was used for OTA detection (Fig. 2c).

Under the optimized conditions, the self-assembling time and temperature for the triple-helix was analyzed. In Fig. 2d, The fluorescent signal decreased gradually, and the self-assembly of AFDNA and QDNA could finish in 10 min with the lowest stable signal. Temperature would affect the formation of the triple-helix aptaswitch and had a knock-on effect on the recognation efficiency of the aptaswitch. When incubated the aptaswitch in the designed temperature (20–45 °C) for 45 min, we found 20, 25, 30 and 37 °C were all beneficial for the stabilization of triple-helix aptaswitch (Fig. S10 in the SI). Together, the self-assembling time of 10 min and temperature of 20–37 °C were chosen to guarantee that the aptaswitch was fully formed.

Additionally, the recognition time between OTA and triple-helix aptaswitch was also investigated. As shown in Fig. 2e, the increasing rate (IR) of signal intensity rose obviously and became stable at around 50 min. This result indicated 50 min was appropriate for the recognition of the aptaswitch with the disassembling of triple-helix structure.

As mentioned above, the temperature was also important in the OTA recognition event. If the temperature was too low, the triple-helix aptaswitch may not be easily dissociated with strong and stable structure, which prevented the recognition of the aptaswitch and OTA. Therefore, we evaluated the influence of recognition temperature for the aptaswitch (20 °C–37 °C). As expected, 37 °C brought the best increasing rate of signal intensity (Fig. 2f). Together, we chose 37 °C for both of aptaswitch self-assembling and OTA recognition.

Since pH of the buffer influenced the stability of the Hoogsteen base pairing and the affinity of the aptamer towards OTA [18,34], pH of binding buffer was optimized (pH 5.0 to 8.0). Finally, the results showed that pH 6.5 was most suitable for the triple-helix aptaswitch in the OTA platform (Fig. S11 in the SI).

### 2.4. Analytical performance of the aptaswitch

Under the optimized conditions, the analytical performance of the aptaswitch was evaluated by introducing different concentrations of OTA from 5 ng/mL to 32 μg/mL. As shown in Fig. 3a, the fluorescent signal was enhanced with the addition of OTA, indicating that the triple-helix aptaswitch was disassembled and the quenched fluorescence

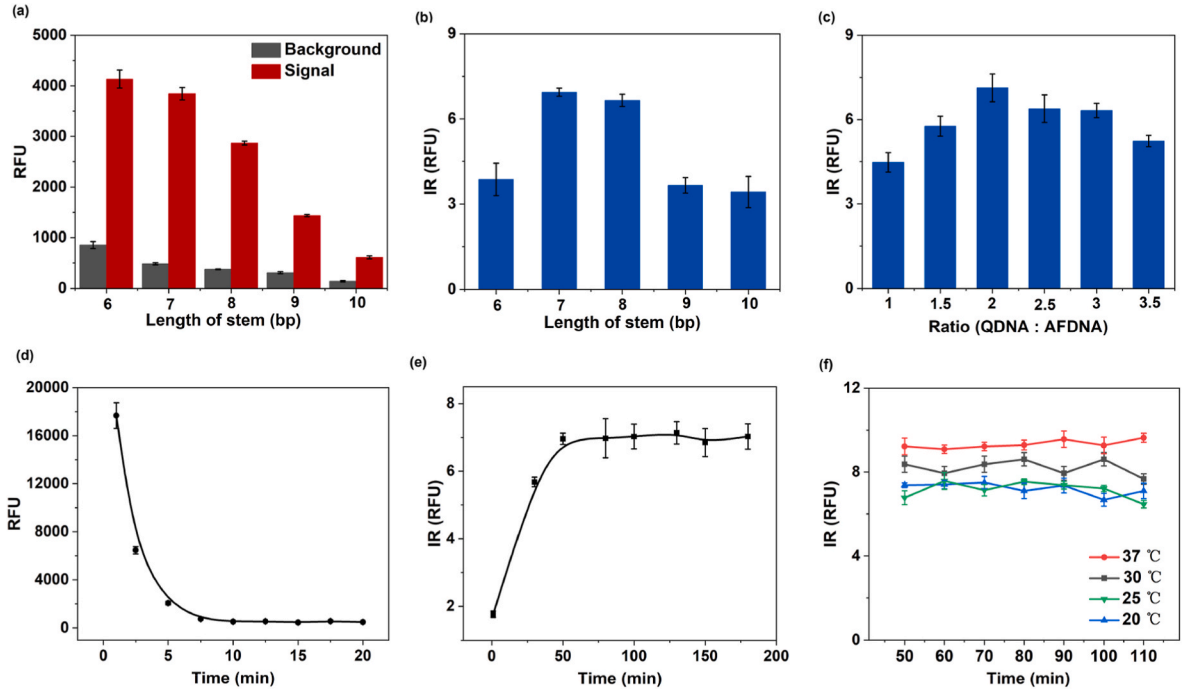


**Fig. 2.** Optimization of the aptaswitch condition. The effect of triple-helix stem length (a, b), ratio of QDNA to AFDNA (c), triple-helix self-assembling time (d), target recognition time (e) and temperature (f) on the increasing rate of arbitrary fluorescence units (IR(RFU)).

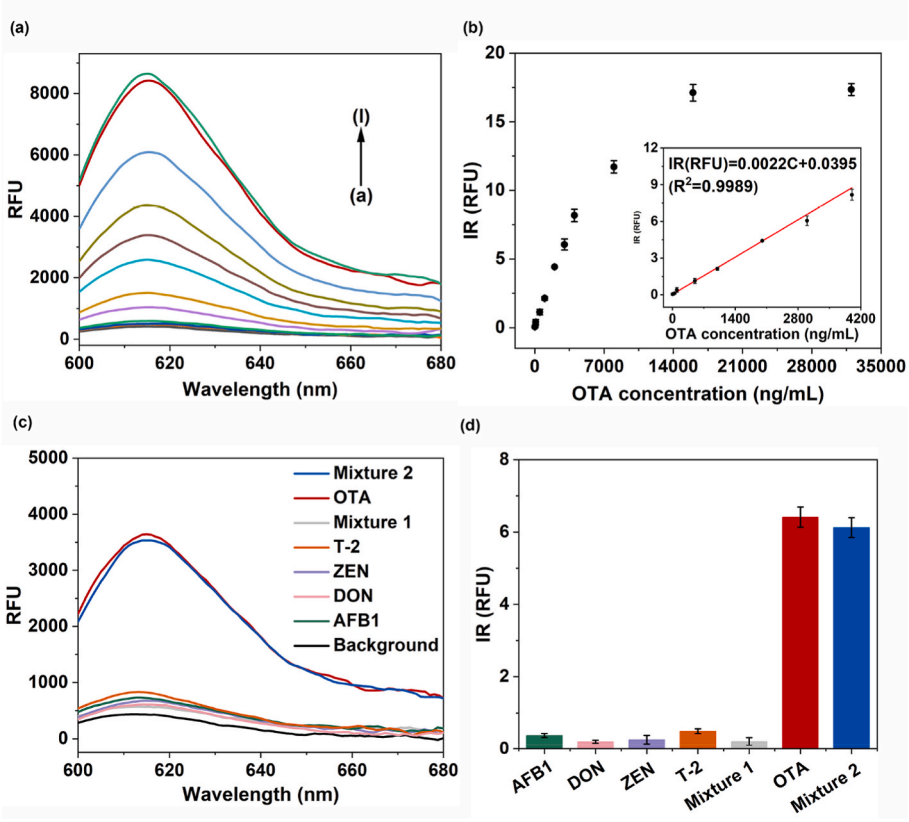


**Fig. 3.** (a) Fluorescence spectra of the aptaswitch with different concentrations of OTA. (Curves a–l: 0, 5, 50, 100, 500, $1 \times 10^3$, $2 \times 10^3$, $3 \times 10^3$, $4 \times 10^3$, $8 \times 10^3$, $1.6 \times 10^4$ and $3.2 \times 10^4$ ng/mL). The increasing rates (IR) of fluorescence intensity at 615 nm was quantified in (b). Linear range: 5 ng/mL-4 μg/mL, LOD: 2.83 ng/mL (3σ/k). (c) Selectivity assay of the aptaswitch. The mixture 1 contained AFB1, DON, ZEN, and T-2. The mixture 2 contained OTA besides mixture 1. The increasing rates (IR) of fluorescence intensity at 615 nm was quantified in (d).

gradually regained. The quantitative calibration for the target concentrations ranging from 5 ng/mL to 4 μg/mL was IR(RFU) = 0.0022C + 0.0395 with the $R^2$ of 0.9989 (Fig. 3b). The limit of detection (LOD) was calculated to be 2.83 ng/mL (3σ/k), below the maximum acceptable safe levels of 3 ng/mL in cereals set by the Commission Regulation (EU) [5].

In order to evaluate the selectivity of the triple-helix aptaswitch, four other mycotoxins at the same concentration with OTA were introduced. As shown in Fig. 3c and d, there were small changes of the fluorescence recovery for the other mycotoxins and their mixture (mixture 1). However, when an individual OTA or a mixture including OTA (mixture 2) were added, we found both resulted in evident response signals. Therefore, with an OTA aptamer serving as the recognition element in the loop of the triple-helix, the developed aptaswitch presented high selectivity toward OTA, which possessed great potential in OTA analysis and quantification.

### 2.5. Bioorthogonal capture of the OTA-AFDNA complex released in the aptaswitch

In this section, the GST-TR512 fusion protein functionalized paper was integrated in the aptaswitch for the signal amlification (Fig. 4a). The signal of red value (R) was digitally quantified from the functionalized paper for the bioorthogonal capture ability to the OTA-AFDNA complex in the aptaswitch (Fig. 4b). When 500 μL of the aptaswitch solution was filtered through, the linear range was 0.1 ng/mL-100 ng/mL with the equation of $\Delta R^{-1} = 0.0489C^{-1}+0.0067$ ($R^2 = 0.9992$) (Fig. 4c). The limit of detection (LOD) was estimated to be 0.091 ng/mL. In the meantime, when the detection volume was 800 μL, the detection range narrowed to 0.03 ng/mL-50 ng/mL with the equation of $\Delta R^{-1} = 0.0149C^{-1}+0.0062$ ($R^2 = 0.9977$) and the detection limit was 0.026 ng/mL (Fig. 4d). The analytical performances of previously reported aptamer-based methods for the detection of OTA were listed in Table S2 in the SI. The linear range and detection limit of the present study were comparable with these existing methods, and even better than most of them. In addition, this detection format did not require complex experimental set-ups (like fluorescence plate reader) or tedious material modification steps for signal amplification. Detections could be performed in a "mix-then-drop" way, which was a simple and cost-effective detection method for OTA.

What's more, as shown in Fig. 4e, the increasing rate (IR) of R value was 1.84 for 5 ng/mL OTA and 4.01 for 50 ng/mL OTA when the detection volume was 500 μL on the functionalized paper, and the IR of the signal enhanced to 3.30 and 4.63 when the volume increased to 800 μL respectively. By contrast, the increasing rate of fluorescence intensity (IR(RFU)) in the aptaswitch solution was only 0.05 and 0.14 for 5 ng/mL and 50 ng/mL OTA (Fig. 3a, b and Fig. 4e). The improved performance was attributed to the bioorthogonal capture-based signal amplification strategy of the functionalized paper, which improved the sensitivity of the aptaswitch remarkably.

### 2.6. Bioorthogonal capture ability of the functionalized paper and the general applicability of the biosensor

To validate the bioorthogonal capture ability of the GST-TR512 fusion protein functionalized paper, we prepared other kinds of papers including denatured protein modified paper and untreated paper for the capture of OTA-AFDNA complex. As seen in Fig. S12a in the SI, these negligible signal improvements indicated the functionality of fusion protein was crucial for the bioorthogonal capture of Texas red fluorophore labeled oligonucleotide.

Subsequently, the positions of fluorophore and quencher were exchanged. There was unbiased capture of fluorophore labeled oligonucleotide by the functionalized paper, and the detection limit was 0.087 ng/mL similar to 0.091 ng/mL developed above when the detection volume was 500 μL (Fig. S12b in the SI and Fig. 4c). What's more, the general applicability of this detection method was also validated by replacing the aptamer sequence in the loop of triple-helix aptaswitch for the small target molecule tetracycline (Kd = 1.067 nM

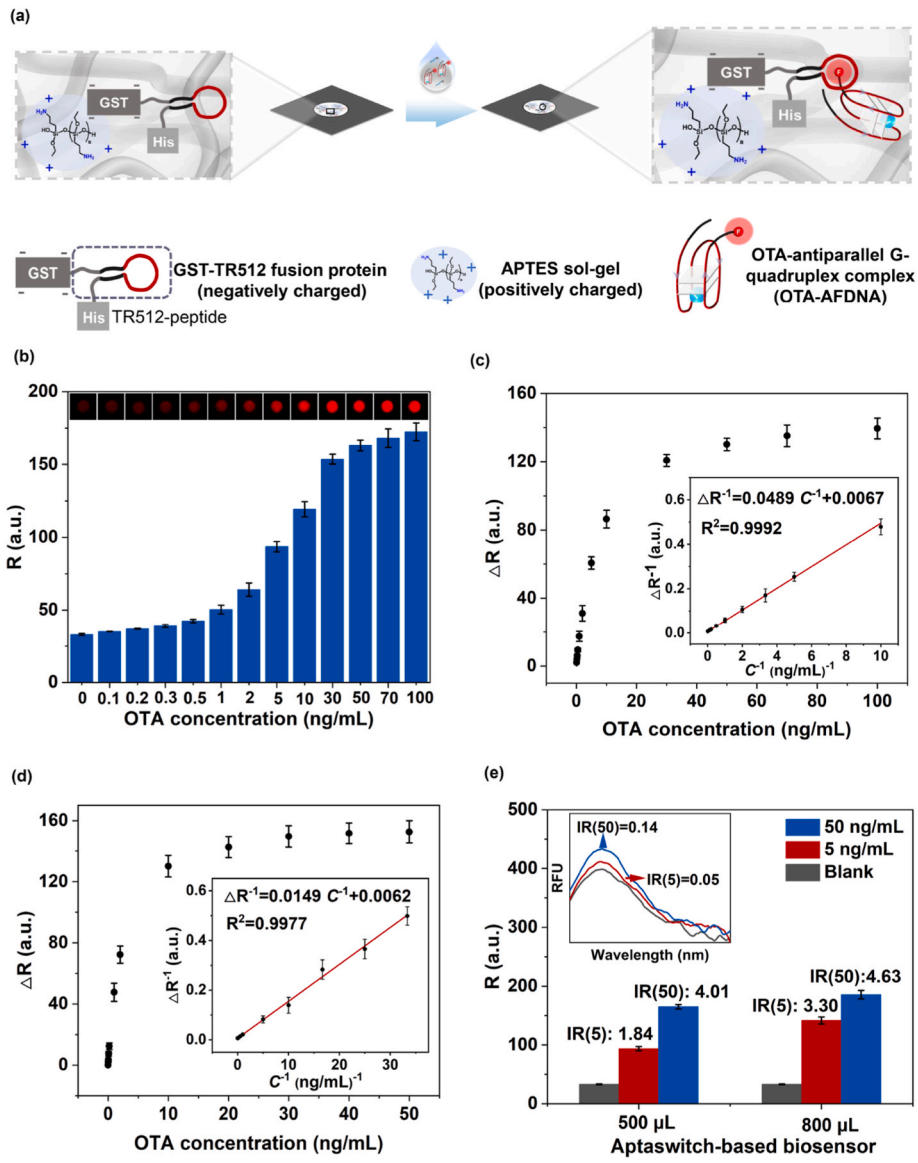


**Fig. 4.** The analytical performance of the functionalized paper in the biosensor. (a) The bioorthogonal capture ability of the GST-TR512 fusion protein functionalized paper. (b) Red value (R) of the functionalized paper with different concentrations of OTA when the detection volume was 500 μL. Insert: The fluorescence picture of the functionalized papers. (c) Calibration plot of the ΔR value as a function of the concentrations of OTA (500 μL). Linear range: 0.1–100 ng/mL, LOD: 0.091 ng/mL (3σ/k). (d) Calibration plot of the ΔR value as a function of the concentrations of OTA (800 μL). Linear range: 0.03–50 ng/mL, LOD: 0.026 ng/mL (3σ/k). (e) The comparison of the increasing rate (IR) of the signals for the detection of 5 ng/mL and 50 ng/mL OTA using different methods (the inset was the result of the detection in the aptaswitch solution and the bar graph was the result of the detection with the functionalized paper in the biosensor). (For interpretation of the references to color in this figure legend, the reader is referred to the Web version of this article.)

[35], Fig. S13 in the SI). Together, we have demonstrated that this aptaswitch-based biosensor was general applicability no matter where the fluorophore was and could be applied to monitor various molecules by replacing the aptamer sequence in the loop of the aptaswitch instead of redesigning the triple-helix structure.

### 2.7. Detection of OTA in real samples

To further investigate the practical feasibility of the biosenser, we applied it in different spiked corn meal samples and peanut samples which were purchased from local supermarket. As shown in Table 1, when the spiked samples were 1 ng/mL to 20 ng/mL, the relative standard derivations were 1.86%–4.49%, and the recoveries were in the range of 99.38%–103.93% with the detection volume of 500 μL on the functionalized paper. These results confirmed that this biosensor could be applied to the quantitative determination of OTA in real samples, with great potential in high accuracy for agricultural products quality monitoring.

**Table 1**
Determination of OTA in real samples[a].

| Samples | Add (ng/mL) | Found (ng/mL) | RSD (%) | Recovery (%) |
|---|---|---|---|---|
| Corn | 1 | 1.02 | 4.49 | 102.00 |
| | 5 | 5.20 | 4.14 | 103.93 |
| | 10 | 9.95 | 2.64 | 99.53 |
| | 15 | 15.33 | 1.86 | 102.20 |
| | 20 | 19.88 | 2.06 | 99.38 |
| Peanut | 1 | 0.99 | 3.49 | 99.49 |
| | 5 | 5.13 | 1.96 | 102.60 |
| | 10 | 10.11 | 1.95 | 101.10 |
| | 15 | 15.16 | 3.84 | 101.06 |
| | 20 | 19.95 | 2.63 | 99.76 |

[a] The data reported in the table represented the average of triplicate measurements.

### 2.8. Design of a hand-held OTA detection device

In addition, we formulated a portable hand-held device for the easy readout of the fluorescent signal on the functionalized paper, which was consisted of a light-emitting diode (LED), two filters and a CCD camera (Fig. 5). With the portable device, we expect that this biosensor may offer a new aptamer-based protocol in point-of-care detection of OTA.

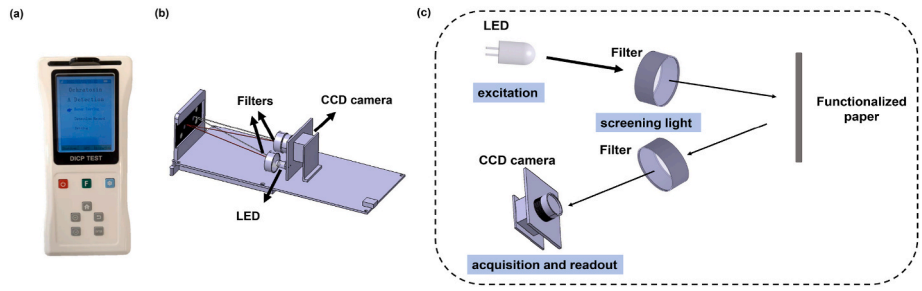


**Fig. 5.** (a) The integrated design of a portable hand-held device. (b) The interior structure of the device, including a LED, two filters and a CCD camera. (c) Working diagram of the detection device.

## 3. Conclusion

In summary, we have developed a sensitive biosensor for OTA detection, which combined the structure-switching of the triple-helix aptaswitch and bioorthogonal capture-based signal amplification of the functionalized paper dexterously. With the presence of the targets, the aptaswitch formed an "open" configuration, generating a substantially increasing fluorescence intensity. Moreover, when the GST-TR512 fusion protein functionalized paper was introduced, the bioorthgonal capture of the Texas red fluorophore labeled oligonucleotide (namely OTA-AFDNA complex) on the functionalized paper released during the OTA-aptamer binding event improved the performance of the aptaswitch remarkably. The obtained aptaswitch-based biosensor showed a detection limit of 0.026 ng/mL with a linear range of 0.03–50 ng/mL when the detection volume was 800 μL. Furthermore, the biosensor was applied to the quantitative determination of OTA in real samples and a portable device was developed for the easy readout of the fluorescent signal in the biosensor. Notably, the biosensor was simple and cost-effective due to the thorough avoidance of fluorescence plate reader or complex material modification steps for signal amplification. At the same time, this general applicable approach could be applied to monitor various molecules by replacing the aptamer sequence in the loop of the aptaswitch without redesigning the triple-helix structure. Hence, such simple, cost-effective and sensitive biosensor could be potentially applied in practical application of OTA quality monitoring, and may offer a new approach to the detection of other small molecule analytes, broadening applications in food safety-related fields.

## CRediT authorship contribution statement

**Mingzhen Zhu:** Conceptualization, Data curation, gave the conceptualization, performed the experiments and data curation, as well as prepared the manuscript. **Wei Yang:** Formal analysis, Writing – review & editing, gave the formal analysis and experimental advice during the process of triple-helix aptaswitch construction. **Hui Zhi:** Writing – review & editing, assisted with the manuscript review and editing. **Changxin Huangfu:** Writing – review & editing, assisted with the manuscript review and editing. **Xiaobo Zhang:** Validation, gave the validation and contributed to the discussion. **Liang Feng:** Formal analysis, designed the experiments and made contribution in funding acquisition. All authors read and approved the manuscript.

## Declaration of competing interest

The authors declare that they have no known competing financial interests or personal relationships that could have appeared to influence the work reported in this paper.

## Data availability

Data will be made available on request.

## Acknowledgments

This work was supported by Key Project of CAS (Grant: KFJ-STS-ZDTP-083) and CAS scientific instruments and equipment development program (Grant: YJKYYQ20200008).

## Appendix A. Supplementary data

Supplementary data to this article can be found online at https://doi.org/10.1016/j.aca.2022.340334.

## References

[1] M.J. Sweeney, A.D. Dobson, Mycotoxin production by Aspergillus, Fusarium and Penicillium species, Int. J. Food Microbiol. 43 (1998) 141–158.
[2] S.C. Duarte, A. Pena, C.M. Lino, A review on ochratoxin A occurrence and effects of processing of cereal and cereal derived food products, Food Microbiol. 27 (2010) 187–198.
[3] P. Kumar, D.K. Mahato, B. Sharma, R. Borah, S. Haque, M.M.C. Mahmud, et al., Ochratoxins in food and feed: occurrence and its impact on human health and management strategies, Toxicon 187 (2020) 151–162.
[4] R. Mateo, A. Medina, E.M. Mateo, F. Mateo, M. Jimenez, An overview of ochratoxin A in beer and wine, Int. J. Food Microbiol. 119 (2007) 79–83.
[5] I. Bazin, E. Nabais, M. Lopez-Ferber, Rapid visual tests: fast and reliable detection of ochratoxin A, Toxins 2 (2010) 2230–2241.
[6] R. Imperato, L. Campone, A.L. Piccinelli, A. Veneziano, L. Rastrelli, Survey of aflatoxins and ochratoxin a contamination in food products imported in Italy, Food Control 22 (2011) 1905–1910.
[7] P.D. Andrade, J.L. Gomes da Silva, E.D. Caldas, Simultaneous analysis of aflatoxins B1, B2, G1, G2, M1 and ochratoxin A in breast milk by high-performance liquid chromatography/fluorescence after liquid-liquid extraction with low temperature purification (LLE-LTP), J. Chromatogr. A 1304 (2013) 61–68.
[8] C. Giovannoli, C. Passini, F. Di Nardo, L. Anfossi, C. Baggiani, Determination of ochratoxin A in Italian red wines by molecularly imprinted solid phase extraction and HPLC analysis, J. Agric. Food Chem. 62 (2014) 5220–5225.
[9] H. Valenta, Chromatographic methods for the determination of ochratoxin A in animal and human tissues and fluids, J. Chromatogr. A 815 (1998) 75–92.
[10] E.P. Meulenberg, Immunochemical methods for ochratoxin A detection: a review, Toxins 4 (2012) 244–266.
[11] A. Visconti, A. De Girolamo, Fitness for purpose–ochratoxin A analytical developments, Food Addit. Contam. 22 (Suppl 1) (2005) 37–44.
[12] A. Chen, S. Yang, Replacing antibodies with aptamers in lateral flow immunoassay, Biosens. Bioelectron. 71 (2015) 230–242.
[13] R. Sharma, K.V. Ragavan, M.S. Thakur, K.S. Raghavarao, Recent advances in nanoparticle based aptasensors for food contaminants, Biosens. Bioelectron. 74 (2015) 612–627.
[14] S.Y. Toh, M. Citartan, S.C. Gopinath, T.H. Tang, Aptamers as a replacement for antibodies in enzyme-linked immunosorbent assay, Biosens. Bioelectron. 64 (2015) 392–403.
[15] M.N. Stojanovic, P.d. Prada, D.W. Landry, Aptamer-based folding fluorescent sensor for cocaine, J. Am. Chem. Soc. 123 (2001) 4928–4931.
[16] X. Wang, Y. Shan, M. Gong, X. Jin, l. Lv, M. Jiang, et al., A novel electrochemical sensor for ochratoxin A based on the hairpin aptamer and double report DNA via multiple signal amplification strategy, Sens. Actuators, B 281 (2019) 595–601.
[17] J. Zheng, A. Jiao, R. Yang, H. Li, J. Li, M. Shi, et al., Fabricating a reversible and regenerable Raman-active substrate with a biomolecule-controlled DNA nanomachine, J. Am. Chem. Soc. 134 (2012) 19957–19960.
[18] J. Zheng, J. Li, Y. Jiang, J. Jin, K. Wang, R. Yang, et al., Design of aptamer-based sensing platform using triple-helix molecular switch, Anal. Chem. 83 (2011) 6586–6592.
[19] A. Verdian-Doghaei, M.R. Housaindokht, K. Abnous, A fluorescent aptasensor for potassium ion detection-based triple-helix molecular switch, Anal. Biochem. 466 (2014) 72–75.

[20] H. Wang, Y. Zhang, H. Ma, X. Ren, Y. Wang, Y. Zhang, et al., Electrochemical DNA probe for Hg(2+) detection based on a triple-helix DNA and multistage signal amplification strategy, Biosens. Bioelectron. 86 (2016) 907–912.
[21] E. Xiong, Z. Li, X. Zhang, J. Zhou, X. Yan, Y. Liu, et al., Triple-helix molecular switch electrochemical ratiometric biosensor for ultrasensitive detection of nucleic acids, Anal. Chem. 89 (2017) 8830–8835.
[22] Y. Wang, Z. Fang, G. Ning, S. Mao, Y. Wu, S. Wu, et al., G-quadruplex-bridged triple-helix aptamer probe strategy: a label-free chemiluminescence biosensor for ochratoxin A, Sens. Actuators, B 298 (2019), 126867.
[23] J.A. Cruz-Aguado, G. Penner, Determination of ochratoxin A with a DNA aptamer, J. Agric. Food Chem. 56 (2008) 10456–10461.
[24] K. He, L. Sun, L. Wang, W. Li, G. Hu, X. Ji, et al., Engineering DNA G-quadruplex assembly for label-free detection of Ochratoxin A in colorimetric and fluorescent dual modes, J. Hazard Mater. 423 (2022), 126962.
[25] L. Huang, J. Wu, L. Zheng, H. Qian, F. Xue, Y. Wu, et al., Rolling chain amplification based signal-enhanced electrochemical aptasensor for ultrasensitive detection of ochratoxin A, Anal. Chem. 85 (2013) 10842–10849.
[26] S. Xie, Y. Chai, Y. Yuan, L. Bai, R. Yuan, Development of an electrochemical method for Ochratoxin A detection based on aptamer and loop-mediated isothermal amplification, Biosens. Bioelectron. 55 (2014) 324–329.
[27] Y. Du, S. Dong, Nucleic acid biosensors: recent advances and perspectives, Anal. Chem. 89 (2017) 189–215.
[28] D.L. Ma, W. Wang, Z. Mao, C. Yang, X.P. Chen, J.J. Lu, et al., A tutorial review for employing enzymes for the construction of G-quadruplex-based sensing platforms, Anal. Chim. Acta 913 (2016) 41–54.
[29] M. Zhu, C. Huangfu, W. Wan, M. Wang, H. Lv, X. Zhang, et al., A novel virus detection strategy enabled by TR512-peptide-based bioorthogonal capture and enrichment of preamplified nucleic acid, Anal. Chem. 94 (2022) 5591–5598.
[30] E. Bagheri, K. Abnous, M. Alibolandi, M. Ramezani, S.M. Taghdisi, Triple-helix molecular switch-based aptasensors and DNA sensors, Biosens. Bioelectron. 111 (2018) 1–9.
[31] K.M. Marks, M. Rosinov, G.P. Nolan, In vivo targeting of organic calcium sensors via genetically selected peptides, Chem. Biol. 11 (2004) 347–356.
[32] M.R. Rajeswari, DNA triplex structures in neurodegenerative disorder, Friedreich's ataxia, J. Biosci. 37 (2012) 519–532.
[33] P. Balagurumoorthy, S.K. Brahmachari, D. Mohanty, M. Bansal, V. Sasisekharan, Hairpin and parallel quartet structures for telomeric sequences, Nucleic Acids Res. 20 (1992) 4061–4067.
[34] R. Nutiu, Y. Li, Structure-switching signaling aptamers, J. Am. Chem. Soc. 125 (2003) 4771–4778.
[35] Y.S. Kwon, N.H. Ahmad Raston, M.B. Gu, An ultra-sensitive colorimetric detection of tetracyclines using the shortest aptamer with highly enhanced affinity, Chem. Commun. 50 (2014) 40–42.